CNS Neuroscience & Therapeutics

ORIGINAL ARTICLE

CNS Neuroscience & Therapeutics

Increasing the Permeability of the Blood–brain Barrier in Three Different Models *in vivo*

Wei-Ye Liu,[1] Zhi-Bin Wang,[1] Yue Wang,[2] Ling-Chang Tong,[1] Ya Li,[1] Xin Wei,[1] Ping Luan[3] & Ling Li[1]

1 Department of Pharmacology, College of Pharmacy, Second Military Medical University, Shanghai, China
2 College of Pharmacy, Ningxia Medical University, Yinchuan, China
3 Medical School, Shenzhen University, Shenzhen, China

Keywords
Animal model; Blood–brain barrier; Tight junction; Vascular permeability.

Correspondence
L. Li, Department of Pharmacology, Second Military Medical University, Shanghai 200433, China.
Tel.: +8621-81871270;
Fax: +8621-65493951;
E-mail: lingli_z163@163.com
and
P. Luan, Medical School, Shenzhen University, Shenzhen 518060, China.
Tel.: +86-755-26958869;
Fax: +86-755-86671906;
E-mail: pingluan01@163.com
Received 30 March 2015; revision 15 April 2015; accepted 17 April 2015

SUMMARY

Aims: Blood–brain barrier (BBB) plays significant roles in the circumstance maintains for the central nervous system (CNS). The dysfunction of the BBB could occur in all pathological conditions of CNS diseases, such as ischemic stroke, cerebral edema, or inflammatory disorders. However, the comparisons among different animal models with a broken BBB *in vivo* are still need to be further studied. **Methods:** Here we used three different mice models *in vivo*, including MCAO induce, LPS treatment, and cold injury to mimic the situation in clinic. The permeability of BBB in three models was detected by perfusion of Evan's blue dye. The functional proteins of the BBB including claudin-5, VE-cadherin, and caveolin-1 were compared in three different models *in vivo*. **Results:** With the hyperpermeability of Evan's blue in the three models, both claudin-5 and VE-cadherin were decreased, while the expression of caveolin-1 was increased. Our study showed that BBB dysfunction induced by MCAO in mice was relatively stable, reliable, and moderate compared with LPS or cold injury-induced BBB permeability models, although the procedural time was generally long and operation complexity was hard. Moreover, our study also found that the model of the increased BBB permeability by cold injury was severe in the regional cerebral tissue and the model treated with LPS was mild in the global cerebral tissue. The operation of the two models *in vivo* was easy, quick, and stable. **Conclusion:** The MCAO model was the most suitable for studying the permeability of BBB among the three models *in vivo*.

doi: 10.1111/cns.12405

Introduction

Blood–brain barrier (BBB) is a dynamic interface between the peripheral blood circulation and the central nervous system (CNS). By avoiding ions and molecules out of the CNS, allowing oxygen and nutrients into the CNS according to the need of the neural cells, BBB sustains a stable environment for the CNS to function well [1,2]. The BBB is formed by the neurovascular unit (including endothelial cells, astrocytes, glia, and neurons), in which the cerebral blood vessels formed by endothelial cells are the core anatomical elements [3]. The endothelial cells in the CNS are unique with that in peripheral tissues, for lacking fenestrations and undergoing extremely low rates of transcytosis [2]. The adherent junctions (AJ) and tight junctions (TJ) between the endothelial cells reflected the paracellular permeability of endothelial cells, while the caveolae reflected the transcellular of the endothelial cells.

The permeability of the BBB increases in almost all CNS diseases, such as ischemic stroke, Parkinson's disease, Alzheimer's disease, amyotrophic lateral sclerosis, epileptic seizures, brain trauma, and diabetes mellitus [4–8]. It remains uncertain whether BBB dysfunction is one of the initial events that lead to the CNS diseases, or whether is a downstream consequence [2]. This needs the development of BBB models in physiological and in pathological conditions. *In vitro* cell-culture-based models of BBB have been greatly developed to predict the permeability of drug candidates. However, the current challenge lies in developing *in vivo* models which retain fundamental BBB characteristics and include difficulty, stability, reproduction, high-throughput capacity, and accurate drug permeability prediction.

Cold injury induces brain trauma with early development of edema and delayed infarction. The injury model displays focal neuronal damage that is similar to the pathological events following head trauma [9–12]. This model is used to study the dynamics of cerebral edema and the time course of BBB breakdown [13]. Ischemic stroke, induced by intraluminal middle cerebral artery occlusion (MCAO) performed in mice, is the second most common cause of death worldwide [14]. After stroke happened, the disruption of BBB could occur continuously [15]. The model has

been widely used to investigate molecular mechanisms of brain injury and potential therapeutic modalities [16]. System inflammation, induced by LPS, could induce cerebrovascular inflammation and injury the BBB [17]. However, only limited information is available on advantage and disadvantage of these BBB models in mice for the research of BBB.

In this study, we performed the three different *in vivo* BBB models which have a hyperpermeable BBB to mimic the pathological conditions in clinic. This study explored Evan's blue extravasation, the expression of TJ protein claudin-5, AJ protein VE-cadherin, and caveolin-1 in BBB dysfunctional model. We compared the differences among these models to provide reference data for future clinical trials and aid investigation of the BBB permeability of other CNS-active substances.

Materials and Methods

Animals

C57BL/6J mice weighing 18–22 g were purchased from SLRC Laboratory Animal Ltd (Shanghai, China). Mice were housed at a controlled temperature of 22 ± 2°C, relative humidity of 50–60% in a 12-h: 12-h light: dark cycle and allowed free access to food and tap water. All animals received humane care, and experimental procedures were performed in accordance with the guidelines of Second Military Medical University for health and care of experimental animals.

Materials

Evan's blue tracer and paraformaldehyde (PFA) were purchased from Sangon biotech (Shanghai, China). Chloral hydrate was purchased from Sinopharm (Shanghai, China). Antibody to VE-cadherin was purchased from Santa Cruz (Dallas, TX, USA), antibody to claudin-5 was purchased from Millipore (Temecula, CA, USA), and antibody to caveolin-1 was purchased from Abcam (Hong Kong, China). Secondary antibodies to Cy3-conjugated anti-rabbit IgG and Alexa Fluor 488 anti-sheep IgG were purchased from Jackson (West Grove, PA, USA). DAPI was purchased from Beyotime (Shanghai, China). Lipopolysaccharides (LPS) from Escherichia coli was purchased from Sigma (St. Louis, MO, USA). 2,3,5-triphenyltetrazolium chloride (TTC) was purchased from Sinopharm (Shanghai, China). Silicon-coated monofilament was purchased from Saixun Co. (Guangzhou, China).

Immunohistochemistry

Immunohistochemical analysis of murine brain tissue was performed to standard produces. Briefly, brains were harvested from skulls after totally perfused with 4% (wt/vol) PFA and then were dehydrated in 30% (wt/vol) sucrose for 48 h. Cryostat sections of 16 um thickness were sliced using a cryostat (Leica, Solms, Germany). Frozen cross sections were incubated with antibodies against caveolin-1 (1:50), claudin-5 (1:50), and VE-cadherin (1:50), respectively, overnight. Secondary antibodies incubated were Cy3-conjugated anti-rabbit IgG (1:200), Alexa Fluor 488 anti-sheep IgG (1:200). The sections were counterstained with DAPI for the nuclei. Images were acquired using Olympus IX71 fluorescence microscope. All pictures in one group were acquired with the same settings.

Animal Models

Cold Injury

The cold injury model was performed similarly as described by Kakinuma et al. [12]. Mice were anesthetized with chloral hydrate in 350 mg/kg and then secured in the stereotactic frame. After that, a longitudinal incision was made starting halfway between the eyes and terminating the ears. The parietal region of

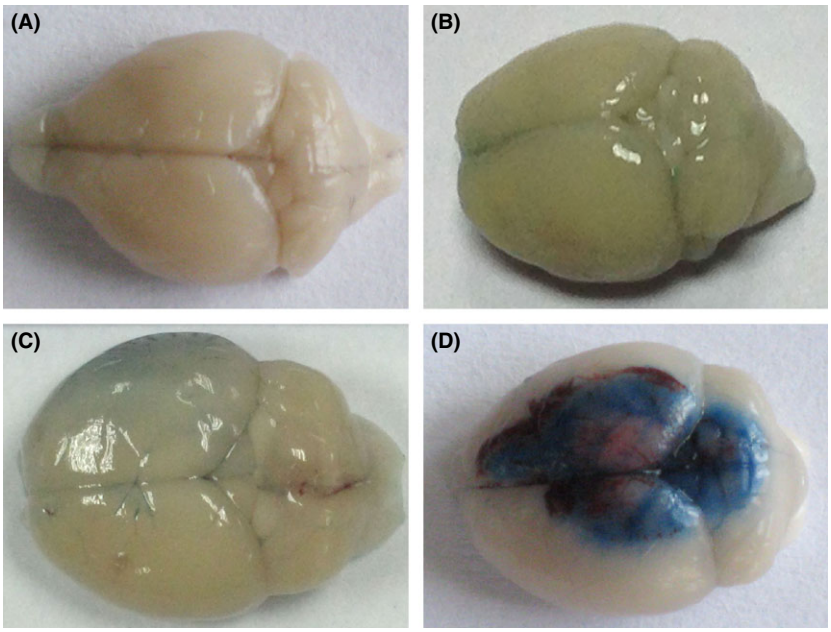

Figure 1 Evan's blue dye penetrated to the BBB in three mice models. (**A**) The brain injected with Evan's blue dye 2 h in normal mice. (**B**) Representative photograph images of the brain with the treatment of LPS 30 mg/kg after Evan's blue dye circulated for 2 h. (**C**) Representative photograph images of the treatment of MCAO for 24 h after Evan's blue dye circulated for 2 h. (**D**) Representative photograph images of the treatment of cold injury after Evan's blue dye circulated for 2 h.

the head was exposed. Then put a 10 g weight in liquid nitrogen, after the temperature kept stable with liquid nitrogen, lay the weights on the skull for 30 seconds. Then the mice were recovered for the next detections.

Middle Cerebral Artery Occlusion (MCAO) Injury

Mice were anesthetized with chloral hydrate in 350 mg/kg. MCAO surgery in mice was performed as described by Koizumi's method [16]. The middle skin incision was made to expose the common carotid artery. A standardized silicon-coated monofilament was inserted into the common carotid artery toward the internal carotid artery until bending was observed or resistance was felt. The core temperature (rectum) was maintained at 37°C ± 0.5°C. The stability of experiments was ensured by the neurological deficits and TTC staining [18].

LPS Treatment Injury

Mice were given a single injection of 30 mg/kg of LPS diluted in saline intraperitoneally.

Evan's Blue Assay in vivo

All animals in three models were injected Evan's blue dye via the vena caudalis in 200 mg/kg 22 h after surgery. After the dye circulating for 2 h, the mice were perfused with normal saline until the colorless liquid flowing from the heart. The brains were harvested for further analyzing. Evan's blue dye could be detected using a 633 nm laser [19]. To further compare Evan's blue dye extracted to the parenchyma of the brain cortex, we detected the specimen cross section under fluorescence microscope. Brains were fixed with 4% paraformaldehyde and then dehydrated for cytoprotection in 30% (wt/vol) sucrose. After the specimens were frozen, 16-μm serial cryostat sections were made for next fluorescence image detection.

Statistical Analysis

All quantified data are presented as mean ± SEM. Image Pro Plus was used to obtain the area of Evan's blue effused in the specimen. We used Student's *t*-test to check for statistical significance between groups. $P < 0.05$ was considered as statistically significance.

Results

Detection of BBB Breakdown by Light Microscopy in Three Animal Models

In order to have a direct observation to the BBB dysfunction in the three different diseases models, we injected Evan's blue dye in

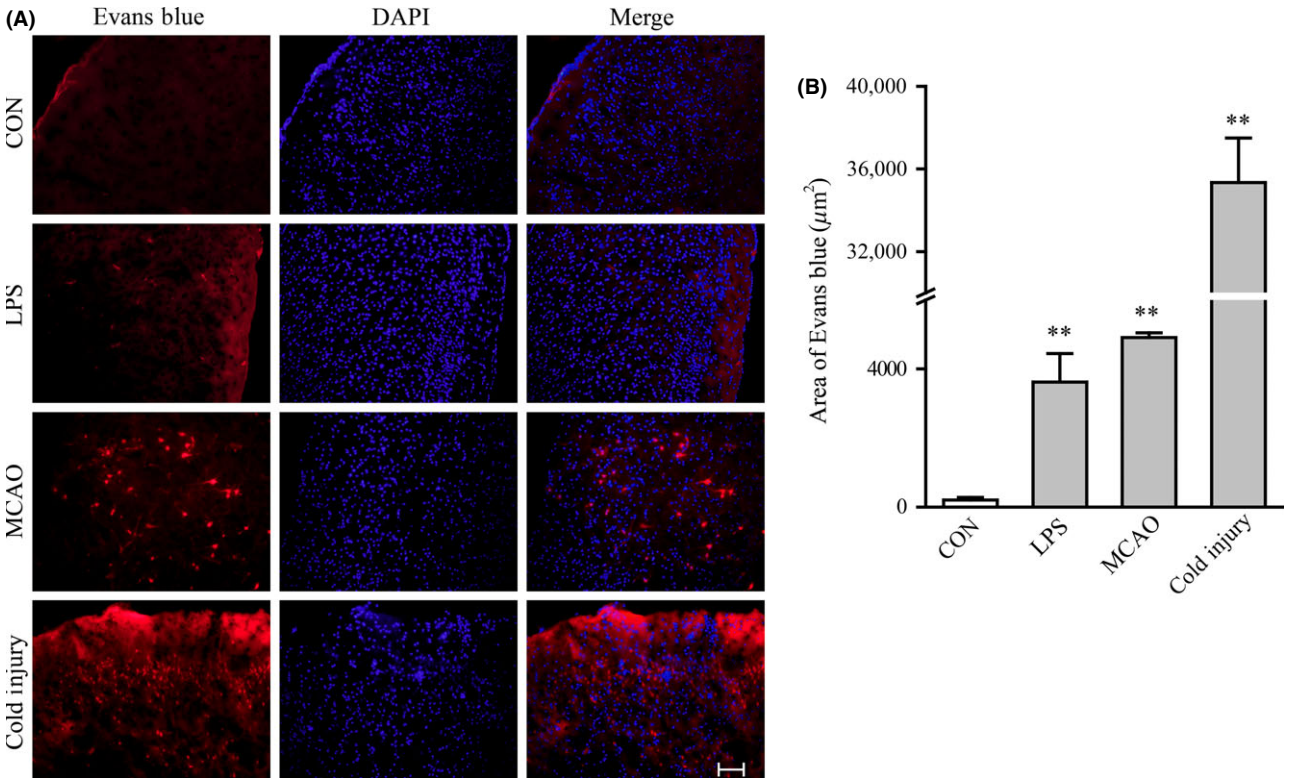

Figure 2 Evan's blue dye penetrates to the BBB detected under fluorescence in mice after three different treatments. (**A**) Representative fluorescence detecting of Evan's blue in control group, LPS treatment group, MCAO treatment group, and cold injury group. The arrow shows the position of Evan's blue dye penetrated. Scale bar, 200 μm. (**B**) Quantitation of Evan's blue dye penetrated through the BBB in three different treatment groups. For each group, n = 7. All the data represent mean ± SEM. *$P < 0.05$ versus control group. **$P < 0.01$ versus control group, determined by Student's *t*-test.

vein to the mice. After 2-h circulation, the mice were sacrificed to harvest the brains. Representative photographs were taken to compare the tracer effusion level directly. In sham group (Figure 1A), the BBB was integrity, and no obvious tracer diffused into the cortex. In the mice treated with LPS 30 mg/kg for 24 h, the degree of diffusion was higher, and the cortex remained in a light blue color in the whole brains (Figure 1B). After MCAO performed 24 h, the permeability of the BBB in the ipsilateral hemisphere was higher than the contralateral hemisphere (Figure 1C). The BBB was dysfunctional in the area contacted to the cold injury, with obvious blue tracer dye infused, while the other part remains inaccessible to the Evan's blue dye (Figure 1D).

Detection of the BBB Breakdown by Fluorescence Microscopy

To further compare Evan's blue dye extracted to the parenchyma of the brain cortex, we detected the specimen cross section under fluorescence microscope. In physical conditions, no obvious Evan's blue dye could be detected in the brain cortex (Figure 2A). In the group of LPS treatment, the dysfunction of the BBB appeared in the whole brain. Clearly tracer infusion could be depicted in the representative photograph. In MCAO model, the extracted tracer was found extracted in the insult zone of ischemic stroke, while the contralateral hemisphere remained normal. In the injury cold model, the effusion of Evan's blue dye was focused on the area of the tissue contacting to the source of cold injury and kept normal in other part of brain tissue, too. The quantitation of the permeability of Evan's blue dye was used to evaluate the BBB dysfunction. Results showed that in the cold injury group, the BBB dysfunction was more serious than that in LPS treatment group and in MCAO group (Figure 2B).

Immunofluorescence Staining Patterns of Standard Proteins

To further investigate the influences of BBB dysfunction on the changes of typical proteins expressed in brain microvascular endothelial cells, the proteins such as claudin-5 (Figure 3), VE-cadherin (Figure 4), and caveolin-1 (Figure 5) were chosen. The expression of claudin-5 in the brain vessels of the cortex decreased with the treatment of LPS for 24 h. At that time, the morphology of vessels was still normal. In MCAO mice model, the morphology of vessels was broken in the insult area. Similar results appeared in the insult area of cold injury. The expression of VE-cadherin in the vessels of the brain cortex decreased after the treatment of LPS. After the performance of MCAO and cold injury, the morphology of vessels could not be detected clearly. Caveolin-1 showed no differences after the treatment of LPS. After the treatment of MCAO, the expression increased in the vessels, while the morphology of the vessels broke down after the treatment of cold injury.

Discussion

It was found in the present study that MCAO model was the most suitable for studying the permeability of BBB among the three

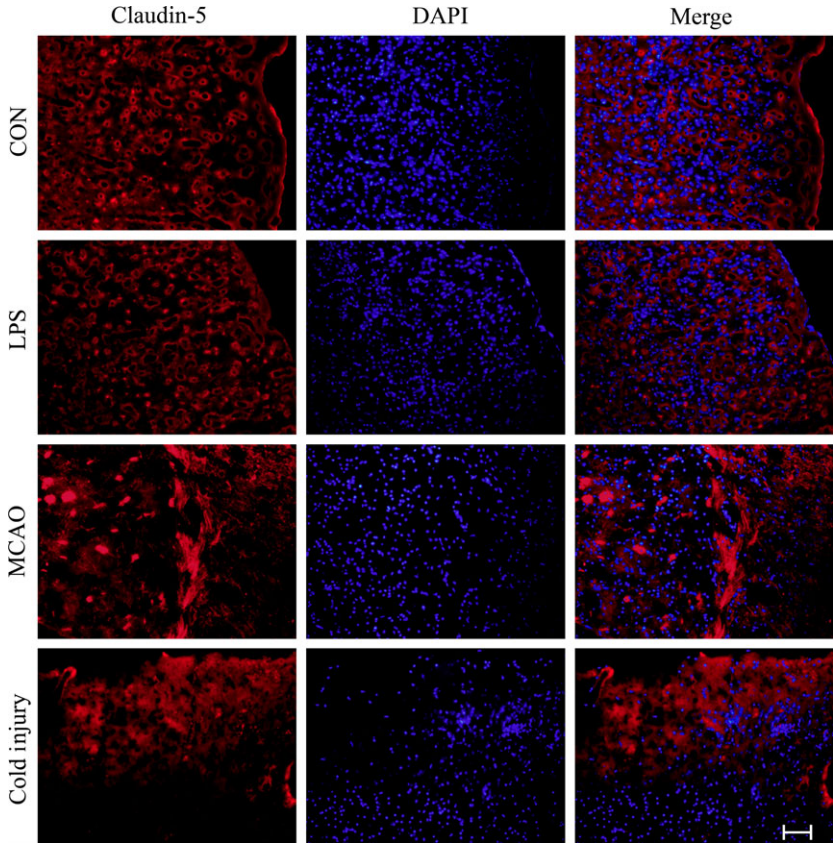

Figure 3 Representative immunofluorescence staining of claudin-5 in the three different treatment groups compared to control. Scale bar, 200 μm. For each group, n = 7. The red shows claudin-5, and the blue shows DAPI.

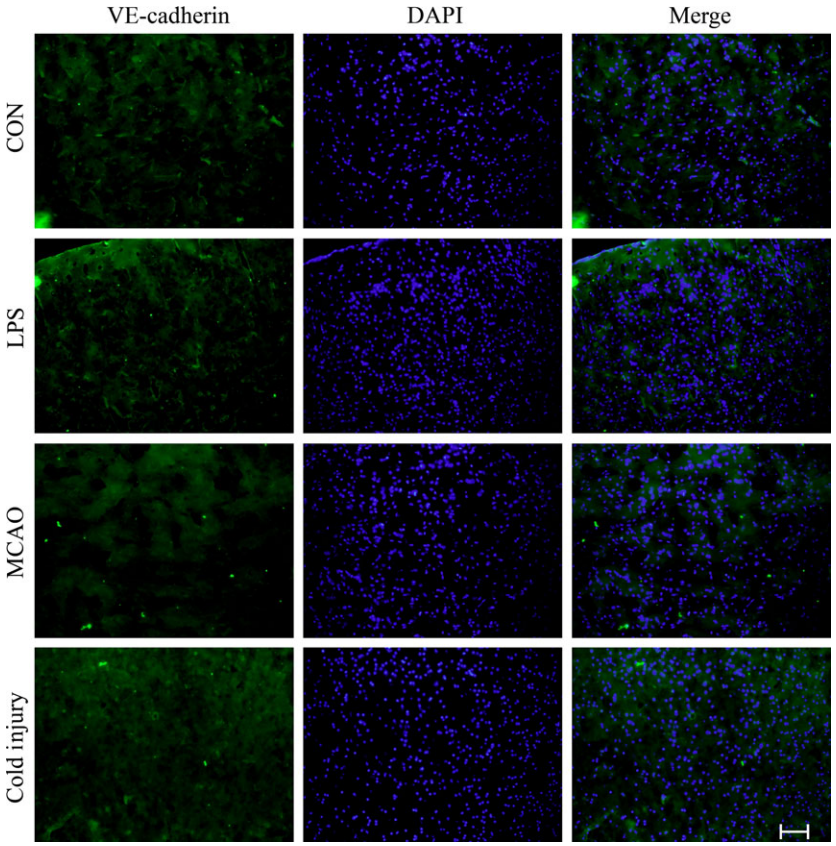

Figure 4 Representative immunofluorescence staining of VE-cadherin in the three different treatment groups compared to control. Scale bar, 200 μm. For each group, n = 7. The green shows VE-cadherin, and the blue shows DAPI.

models *in vivo*. Our study also demonstrated that the expression of claudin-5 and VE-cadherin decreased and caveolin-1 increased, accompanying with the increase of BBB permeability in three models *in vivo*. (Shown in Table 1)

The MCAO model, which replicates focal cerebral ischemia in rodent, has been widely used to study the BBB function. This model has the advantage of inducing reproducible transient or permanent ischemia of the middle cerebral artery territory in a relative noninvasive manner, accompanying with the increase of BBB permeability. The disadvantage of the model lies in many variables, such as strain-related differences, size, length, shape and flexibility of suture tip, duration of occlusion, body temperature, anesthesia, and other factors which can lead to inconsistency in infarct volumes in this model. However, our study showed that BBB dysfunction induced by MCAO in mice was relatively stable, reliable, and moderate compared with LPS or cold injury-induced BBB permeability model, although the procedural time was generally long and operation complexity was hard. Moreover, our study also found that the model of the increased BBB permeability by cold injury was severe in the regional cerebral tissue and the model treated with LPS was mild in the global cerebral tissue. The operation of the two models *in vivo* was easy, quick, and stable. Taken together, the increased BBB permeability in MCAO model is more suitable for study the BBB functions, compared with that in cold injury and LPS-treated models.

The permeability of BBB is mediated by at least two mechanisms: the paracellular pathway and the transcellular pathway. The former is regulated by the opening and closing of endothelial cells, the later includes vesicular transport systems and fenestrae and biochemical transporters [20]. There are two major structures controlling the opening and closing of the BBB, tight junction and adherent junction. In this study, claudin-5 and VE-cadherin were chosen as the representative proteins of TJs and AJs, and caveolin-1 as the representative protein of vesicular transport systems.

Claudin-5 is a critical regulator of BBB permeability. In previous studies, deletion of claudin-5 in mice affected BBB permeability against small molecules beyond 800 Da, as a molecular sieve. Mutant mice without claudin-5 died a few hours after birth [21,22]. In the present study, we found that the expression level of claudin-5 decreased in all the three models. Especially, the morphology of cerebral vessels disrupted in the model of MCAO and cold injury, suggested a more severe dysfunction of BBB in both of the two models.

VE-cadherin is an endothelial-specific cell-to-cell adhesion protein in the AJ, playing a significant role in the control of endothelial cell permeability and integrity [23]. Both the phosphorylation and the cleavage of VE-cadherin could induce vascular permeability [20]. VE-cadherin gene knockout is lethal in mouse embryos, interfering with which in adult mice affects the vascular integrity *in vivo*, and blocking its adhesive function influenced the endothelial barrier maintenance *in vitro* [24]. In our study, we found that the expression of VE-cadherin decreased in the model of MCAO, accompanied with the other two models *in vivo*, too.

Caveolin-1 is a major component of caveolae, mainly expressed in vessels in the CNS [25], and has a role in vesicular

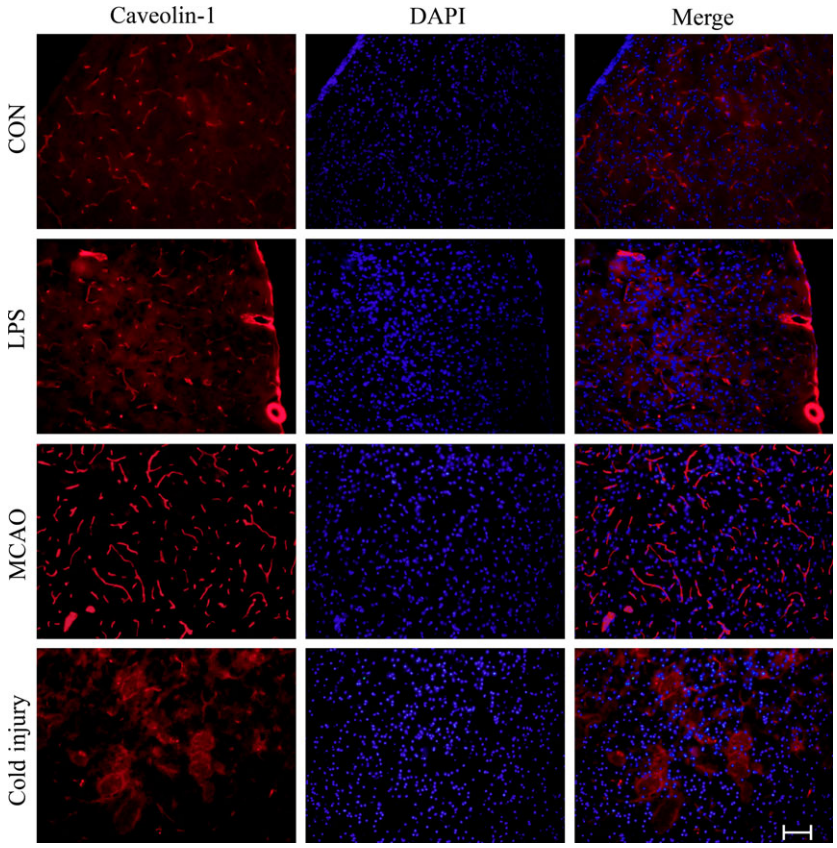

Figure 5 Representative immunofluorescence staining of caveolin-1 in the three different treatment groups compared to control. Scale bar, 200 μm. For each group, n = 7. The red shows caveolin-1, and the blue shows DAPI.

Table 1 Comparison of three methods which damage the BBB permeability in mice

	MCAO	LPS treatment	Cold injury model
Procedural time	Generally longer	Generally quicker	Generally quicker
Operation **c**omplexity	Hard	Easy	Easy
Stability	More stable	Less stable	More stable
Site of BBB breakdown	Local	Global	Local
Severity of BBB dysfunction	Moderate	Mild	Severe
Evans blue's permeability	Moderate	Mild	Severe
Postoperative performance	Circling in a direction	Autonomic activity weakened	Autonomic activity weakened
Molecular level change	Claudin-5↓ VE-cadherin↓ Caveolin-1↑	Claudin-5↓ VE-cadherin↓	Claudin-5↓ VE-cadherin↓ Caveolin-1↑
Mortality rate in 24 h	Low	High	Low
Clinical application	Ischemic stroke	Meningitis	Cerebral edema

trafficking in transcytosis of proteins, endocytosis, and potocytosis [13]. Increased caveolin-1 expression has been found in the experimental autoimmune encephalomyelitis animal model [26]. Similar to Nag's et al. study [13], we also found that the expression of caveolin-1 increased in the cold injury model, and the vessels contacting the liquid nitrogen lost its morphology. Moreover, the expression of caveolin-1 increased in the LPS treatment group and the MCAO group. With the hyperpermeability of Evan's blue in the three diseases animal models, we speculated that the caveolin-1 increased with the BBB dysfunction.

In summary, we chose three representative proteins as molecular explanations of the broken to the BBB, which was coincident with previous studies. Moreover, we compared the complexity and the stability among the three models *in vivo*. Damaging the BBB permeability by MCAO was relatively convenient of manipulation, reliable and moderate BBB model *in vivo* to date, compared with LPS and cold injury-induced dysfunction of the BBB.

Acknowledgments

This work was supported by grants from the National Natural Science Foundation of China (No. 81273504, 81473258 and 81402941) and China Basic Research Program 2009CB521901.

Conflict of Interest

The authors declare no conflict of interest.

References

1. Liu WY, Su DF. Blood-brain barrier is not a barrier in the development of new drugs for ischemic stroke. *CNS Neurosci Ther* 2014;**20**:1013–1014.
2. Obermeier B, Daneman R, Ransohoff RM. Development, maintenance and disruption of the blood-brain barrier. *Nat Med* 2013;**19**:1584–1596.
3. Tam SJ, Watts RJ. Connecting vascular and nervous system development: Angiogenesis and the blood-brain barrier. *Annu Rev Neurosci* 2010;**33**:379–408.
4. Huang JY, Li LT, Wang H, et al. In vivo two-photon fluorescence microscopy reveals disturbed cerebral capillary blood flow and increased susceptibility to ischemic insults in diabetic mice. *CNS Neurosci Ther* 2014;**20**:816–822.
5. Krol S, Macrez R, Docagne F, et al. Therapeutic benefits from nanoparticles: The potential significance of nanoscience in diseases with compromise to the blood brain barrier. *Chem Rev* 2013;**113**:1877–1903.
6. Schoknecht K, Prager O, Vazana U, et al. Monitoring stroke progression: In vivo imaging of cortical perfusion, blood-brain barrier permeability and cellular damage in the rat photothrombosis model. *J Cerebr Blood F Met* 2014;**34**:1791–1801.
7. Lee H, Pienaar IS. Disruption of the blood-brain barrier in Parkinson's disease: Curse or route to a cure? *Front Biosci* 2014;**19**:272–280.
8. Marques F, Sousa JC, Sousa N, Palha JA. Blood-brain-barriers in aging and in Alzheimer's disease. *Mol Neurodegener* 2013;**8**:38.
9. Lok J, Wang XS, Xing CH, et al. Targeting the neurovascular unit in brain trauma. *CNS Neurosci Ther* 2015;**21**:304–308.
10. Chan PH, Longar S, Fishman RA. Protective effects of liposome-entrapped superoxide dismutase on posttraumatic brain edema. *Ann Neurol* 1987;**21**:540–547.
11. Hama H, Kasuya Y, Sakurai T, et al. Role of endothelin-1 in astrocyte responses after acute brain damage. *J Neurosci Res* 1997;**47**:590–602.
12. Kakinuma Y, Hama H, Sugiyama F, et al. Impaired blood-brain barrier function in angiotensinogen-deficient mice. *Nat Med* 1998;**4**:1078–1080.
13. Nag S, Venugopalan R, Stewart DJ. Increased caveolin-1 expression precedes decreased expression of occludin and claudin-5 during blood-brain barrier breakdown. *Acta Neuropathol* 2007;**114**:459–469.
14. Donnan GA, Fisher M, Macleod M, Davis SM. Stroke. *Lancet* 2008;**371**:1612–1623.
15. Moretti R, Pansiot J, Bettati D, et al. Blood-brain barrier dysfunction in disorders of the developing brain. *Front Neurosci* 2015;**9**:40.
16. Ansari S, Azari H, McConnell DJ, Afzal A, Mocco J. Intraluminal middle cerebral artery occlusion (MCAO) model for ischemic stroke with laser doppler flowmetry guidance in mice. *J Vis Exp* 2011;**51**:2879.
17. Denes A, Ferenczi S, Kovacs KJ. Systemic inflammatory challenges compromise survival after experimental stroke via augmenting brain inflammation, blood- brain barrier damage and brain oedema independently of infarct size. *J Neuroinflammation* 2011;**8**:164.
18. Guo JM, Liu AJ, Zang P, et al. ALDH2 protects against stroke by clearing 4-HNE. *Cell Res* 2013;**23**:915–930.
19. Walchli T, Mateos JM, Weinman O, et al. Quantitative assessment of angiogenesis, perfused blood vessels and endothelial tip cells in the postnatal mouse brain. *Nat Protoc* 2015;**10**:53–74.
20. Dejana E, Tournier-Lasserve E, Weinstein BM. The control of vascular integrity by endothelial cell junctions: Molecular basis and pathological implications. *Dev Cell* 2009;**16**:209–221.
21. Matter K, Balda MS. Holey barrier: Claudins and the regulation of brain endothelial permeability. *J Cell Biol* 2003;**161**:459–460.
22. Nitta T, Hata M, Gotoh S, et al. Size-selective loosening of the blood-brain barrier in claudin-5-deficient mice. *J Cell Biol* 2003;**161**:653–660.
23. Harris ES, Nelson WJ. VE-cadherin: At the front, center, and sides of endothelial cell organization and function. *Curr Opin Cell Biol* 2010;**22**:651–658.
24. Gavard J. Endothelial permeability and VE-cadherin: A wacky comradeship. *Cell Adh Migr* 2013;**7**:455–461.
25. Virgintino D, Robertson D, Errede M, et al. Expression of caveolin-1 in human brain microvessels. *Neuroscience* 2002;**115**:145–152.
26. Shin T, Kim H, Jin JK, et al. Expression of caveolin-1, -2, and -3 in the spinal cords of Lewis rats with experimental autoimmune encephalomyelitis. *J Neuroimmunol* 2005;**165**:11–20.

